VECTOR
ANALYSERS

IEE ELECTRICAL MEASUREMENT SERIES 5

Principles of Microwave Measurements

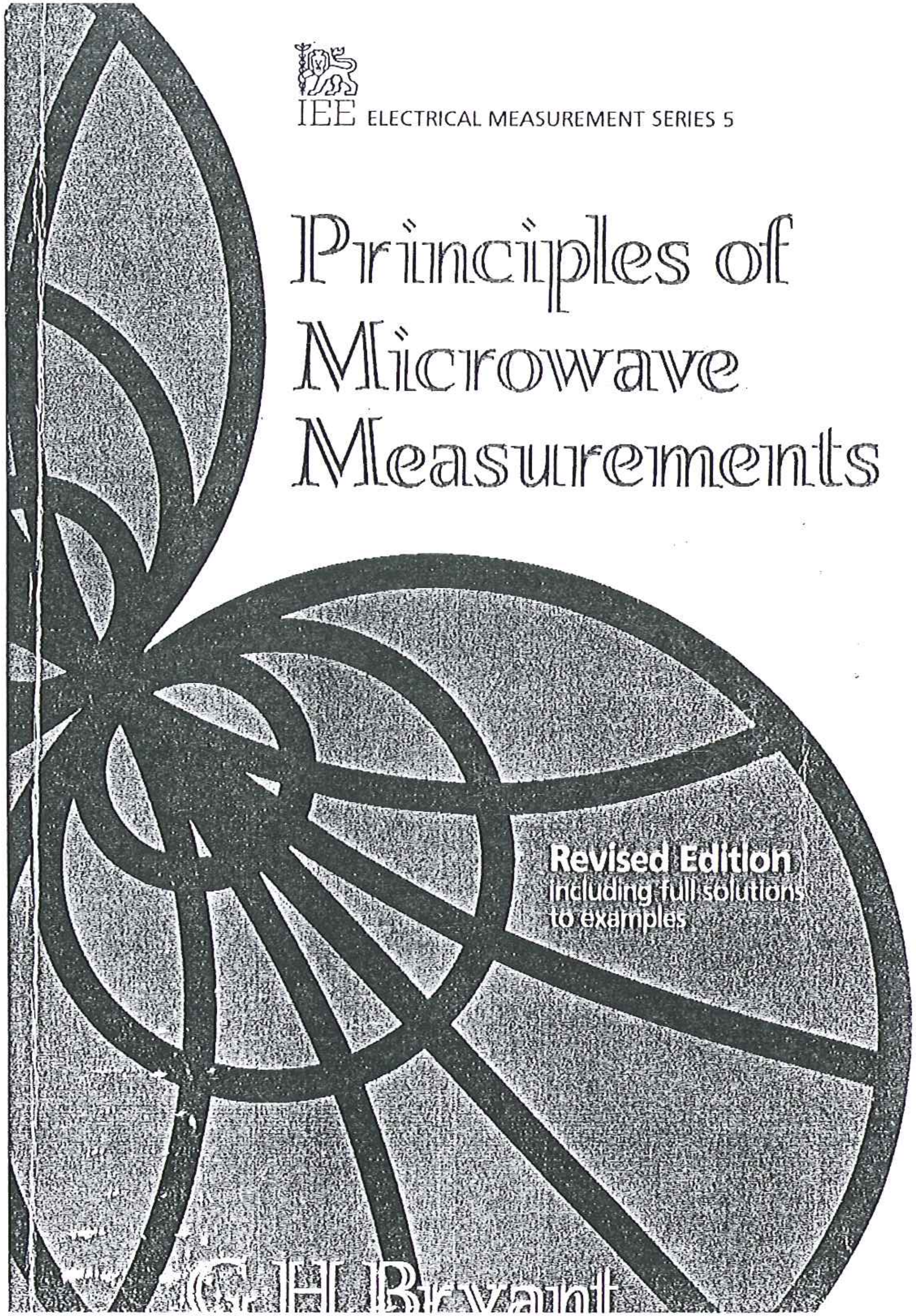

Revised Edition
including full solutions to examples

G H Bryant

Chapter 5

Vector analysers

5.1 Vector measurement systems

Vector analysers measure amplitude and phase of reflected or transmitted signals with respect to an input reference, either directly or as complex ratios. There are many different types of analyser systems, distinguished by their error-correction capabilities, output display, degree of automation etc. A complete vector network system usually has an analyser and test set at its centre, to which is added a display unit, a suitable sweep oscillator, a controlling computer and further items as required by the measurement in progress. For instance, a computer is not always necessary for single measurements; displays are often simple meters etc. This discussion of vector network analysers takes place around a particular example, the Hewlett–Packard HP8510. By choosing an advanced commercially available instrument we are able to subsume the techniques of many other examples in a single description, digressing where necessary to include some important aspects not otherwise covered in the thematic context. By concentrating on modern instrumentation we are ignoring many interesting methods not currently in use. An alternative historical presentation can be found in References 1 and 2.

5.2 The HP8510

The major elements of a measurement system based on the HP8510 are shown[6] in Fig. 5.1. They can be broken into three parts: the source, which is a programmable synthesised sweeper or sweep oscillator; the test set, consisting of a splitter and bridge network for measuring forward and reverse S-parameters of a two-port device under test; and the analyser itself, which in this case includes a control microprocessor, a number of peripherals and access to an external data bus (HP–IB) for remote or automatic operation.

Sweeper scan range and frequency are selected via the analyser's system bus. In each sweep, measurements can be made at 51, 101, 201 or 401 discrete

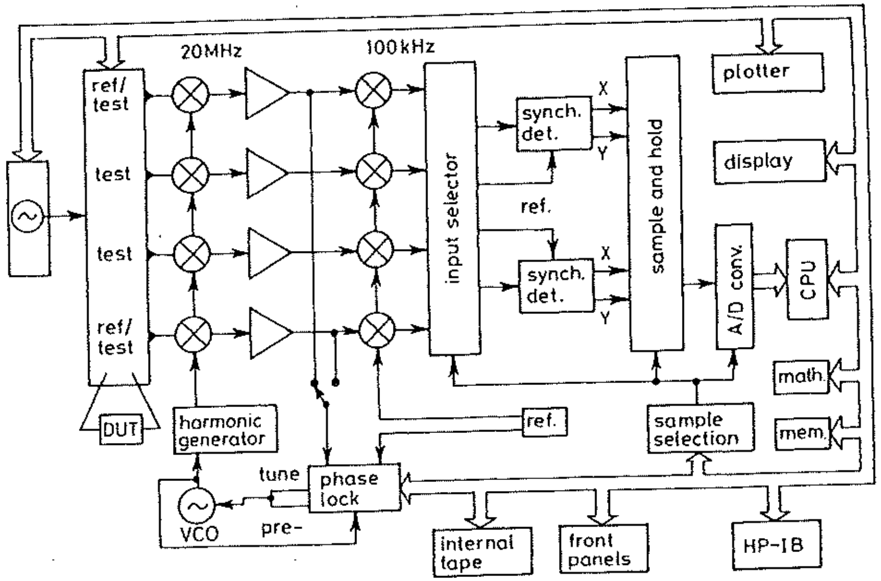

Fig. 5.1 *HP8510 block diagram (After BRAUN, 1984)*

frequencies. The test set is designed to avoid the need to reverse connections to the DUT when reversed signal flow is required. One reference and the two test channels are used to measure transmission and reflection for one signal flow through the DUT. The other reference is similarly used in the reverse direction. Conversion to first IF is made by locking a harmonic of the local oscillator VCO at 20 MHz above the selected reference channel. Tuning of the phase-locked loop is by digital division to ensure precise repetition from sweep to sweep. When the main loop, via the sampling mixer, is unlocked, pretune selects a harmonic by digital control of a second phase-lock loop. The harmonic is chosen to be within the IF bandwidth of the main loop, so that the VCO becomes a signal-tracking oscillator. A common crystal reference serves both phase-lock loops, as well as local oscillator for the second down conversion to 100 kHz. Auto-ranging is achieved by ratioing the test channels with the reference channel and controlling amplifier gains in the input selector to optimise sensitivity for all signal levels. Common-mode variations are also minimised by the same process. A digitally controlled synchronous detection precedes a sample-and-hold multiplier, that in turn drives an analogue/digital convertor. From there the readings enter a central processing unit prior to storage or display. Each reading takes about 40 μs for an analogue/digital conversion, and four readings are made for each data point.

Many of the standard components of the HP8510 are found as optional additions in earlier systems. Complete integration of a 16 bit microprocessor with the analyser and sweeper allows use of a more complex error-correction algorithm, whilst also reducing measurement time compared to other systems. Thus forward and reverse scattering parameters of a network are measured at 401 frequency points in 800 ms, giving virtual real-time operation during network adjustments. Dynamic accuracies of $\pm 0{\cdot}5$ dB and $\pm 0{\cdot}3°$ in amplitude and phase are also claimed.

5.3 Microwave test sets

The S-parameter test set as part of an HP8510 network-analyser system incorporates both transmission and reflection measurements as shown in Fig. 5.2. If we begin with forward testing of a DUT, the input switch connects the RF via the splitter to reference channel a_1 and via a step attenuator in the incident channel to the device under test. A bias TEE, also inserted in the incident (and transmission) channel, is to allow DC biasing on active DUTs. A bridge circuit, similar to a directional coupler, but providing 6 dB or more isolation between any two forward ports, separates the reflected signal into test channel b_1. The transmitted signal is separated from the main channel by a second bridge and directed to test channel b_2. In reverse, signal flow is in the opposite direction through the device with channel a_2 as reference and b_2 and b_1 as reflection and transmission outputs, respectively.

The first IF conversion to 20 MHz is in a sampling mixer with a step-recovery diode as described in Chapter 4. Harmonics are generated from a local-oscillator VCO tuned over a 60—160 MHz range, one of which is locked over

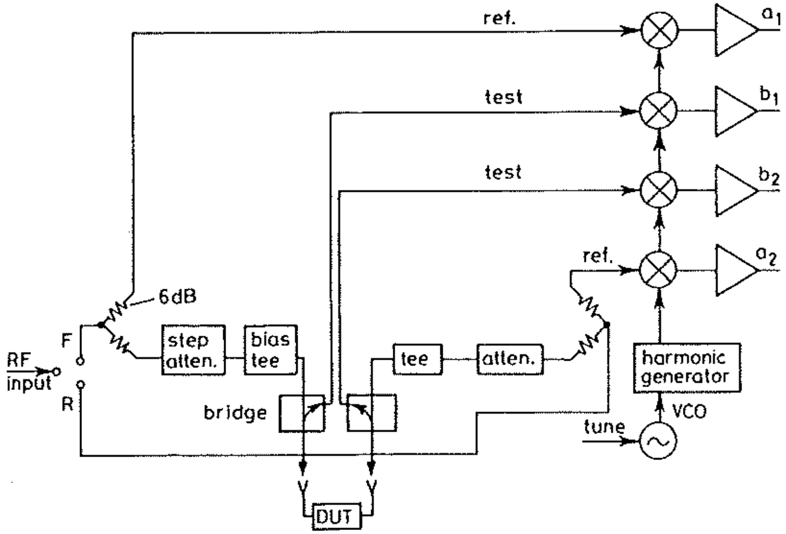

Fig. 5.2 *HP8510 test set (After BRAUN, 1984)*

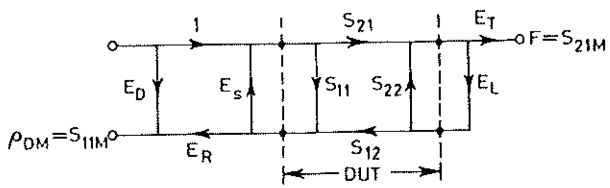

Fig. 5.3 *Error flowgraph for transmission*

an octave range to the incoming signal. Automatic retuning of the local oscillator allows a change of harmonic-number selection for each octave band in the range 45 MHz—26·5 GHz.

Disturbances due to reflections in the test set are kept to a minimum by the 6 dB loss in each arm of the splitters and the effective 12 dB loss for passes through the bridges. Thus, in error-free conditions, reflection measurements give S_{11} and S_{22}, and transmission measurements S_{21} and S_{12}. In the presence of errors, we have already seen in Chapter 2 how an error model for a one-way transmission and reflection measurement can provide insight into error correction by means of known calibration standards. This simple model, repeated in Fig. 5.3, has two deficiencies in that it does not take account of crosstalk between reference and test channels in the mixers, switches and IF amplifiers; and that it also requires the DUT to be reversed in the test set to measure S_{12} and S_{22}. Connector disturbance during reconnection can change some error terms between a forward and reverse run, leading to uncorrectable residual errors. Fig. 5.4 shows how the addition of an extra flow path takes account of transmission leakage crosstalk and Fig. 5.5 extends the model to correspond with a non-reversing or switched test set. The 12-term error model of Fig. 5.5 allows for different directivity errors (E_{DF}, E_{DR}) in the two bridges, crosstalk in both directions (E_{XF}, E_{XR}), different effective source errors (E_{SF}, E_{SR}) and transmission losses (E_{TF}, E_{TR}). By careful attention to the balancing of each pair of components it may sometimes by possible to obviate the need to determine every term. However, for devices with large reflectivities and non-reciprocal components the full model is necessary.

A calibration procedure, with known standards substituting for the DUT, is applied to determine the model error terms. Standards for reflection calibration

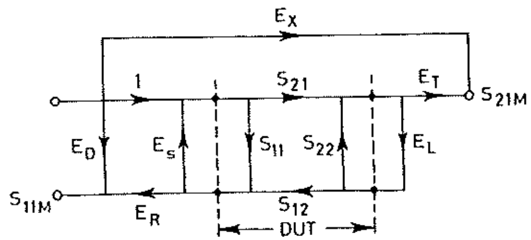

Fig. 5.4 *Six-term error model*

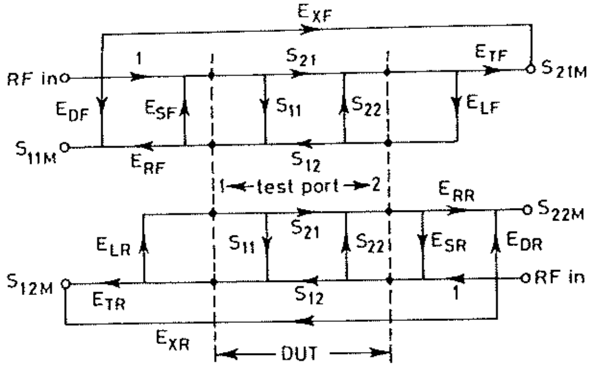

Fig. 5.5 *Twelve-term error model*

are commonly a matched load, a short and an open circuit. They are connected and measured as S_{11} at the two ports, and have equivalent flowgraphs as shown in Fig. 5.6. Their accuracy depends on careful design and maintenance, and on their comparison with national standards at laboratories such as the National Bureau of Standards in the USA or the National Physical Laboratory in the UK. Errors in 'perfect' loads cause small reflections that can be evaluated by placing the load at the end of an accurate sliding air line. Any reflection from the load adds to the directivity error of the test port E_D. By sliding the load on the air line the relative phases of both errors are changed to give the polar plot of Fig. 5.7, when the small reflection δE due to the load adds vectorially to the constant phase vector E_D of the directivity. Since varying air-line length rotates δE about P, a true value for E_D is found by measuring $E_D + \delta E$ at several points around the error circle in order to find its centre.

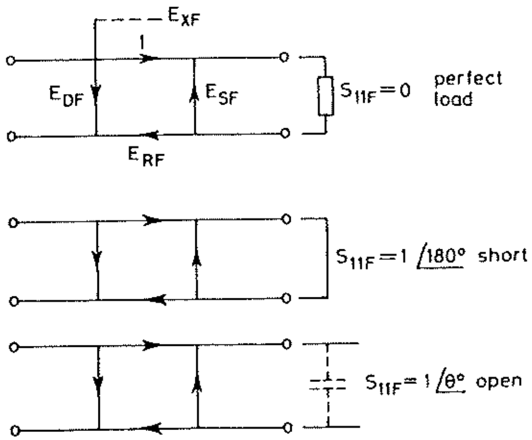

Fig. 5.6 *Calibration loads*

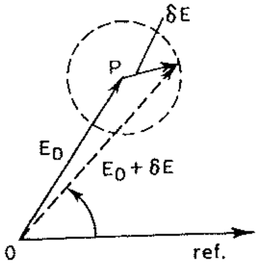

Fig. 5.7 *Sliding-load vector diagram*

Short-circuit standards are limited by connector connection repeatability and open circuits in coaxial line by a small fringing capacitance, that can be accurately modelled as a phase angle θ in Fig. 5.6. In waveguide an offset open circuit can be simulated by a $\lambda/4$ length of shorted waveguide. Connectors are an error source partly influenced by careful operator training. Manufacturers usually give instructions on how to handle connector changes, including cleaning methods to maintain good contacting surfaces. A good 7 mm connector has an S_{11} of -90 to -100 dB with repeatability over a 15 dB range, but adapter connections involving transitions between connector types can seriously degrade performance to less than -30 dB.

To calibrate a test set, each of the calibration terminations is measured at all frequencies in the required scan range. For the sliding load several (4—6) positions of the termination are taken at each frequency, with the operator making connections and adjustments on request from the computer. In the error model of Fig. 5.6, the measured reflection coefficient is

$$S_{11M} = E_{DF} + \frac{S_{11F}E_{RF}}{1 - E_{SF}S_{11F}} \tag{5.1}$$

Three known S_{11F} for forward and S_{22R} for reverse signal flow give three equations for E_{DF}, E_{RF}, E_{SF} and a further three for E_{DR} E_{RR}, E_{SR} with

$$S_{22M} = E_{DR} + \frac{S_{22R}E_{RR}}{1 - E_{SR}E_{22R}} \tag{5.2}$$

For crosstalk, E_{XF} can be determined by making a transmission measurement at port 2 with no connection to either port. Load match and transmission tracking errors, E_{LF} and E_{TF}, follow from measurement of reflection and transmission with a through connection of port 1 to port 2. These cases are represented by the flowgraphs of Figs. 5.8*a* and *b*, respectively. E_{XF} is therefore found directly, but E_{SF} and E_{LF} require two further equations easily derived from the developed flowgraph in Fig. 5.9, by writing

$$S_{11M} = E_{DF} + \frac{E_{RF}E_{LF}}{1 - E_{SF}E_{LF}} \tag{5.3}$$

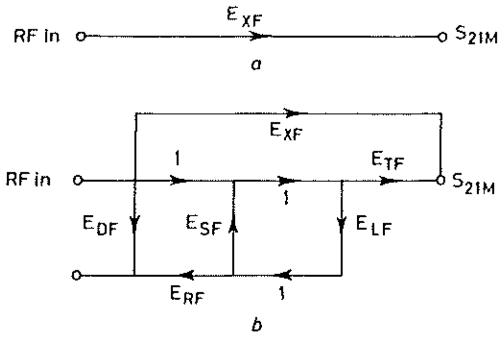

Fig. 5.8 *No-connection and through measurements*

$$S_{21M} = E_{XF} + \frac{E_{TF}}{1 - E_{SF}E_{LF}} \tag{5.4}$$

where S_{11M} and S_{21M} are the measured reflection and transmission coefficients in a forward transmission with a through connection. Transmission-tracking and load-reflection errors follow from the previous equations as

$$E_{TF} = \frac{1}{E_{RF}}\left[\frac{S_{11M} - E_{XF}}{E_{SF}S_{11M} - E_{SF}E_{DF} + E_{RF}}\right] \tag{5.5}$$

$$E_{LF} = \frac{S_{11M} - E_{DF}}{E_{SF}S_{11M} - E_{SF}E_{DF} + E_{RF}} \tag{5.6}$$

Six calibration measurements are necessary, leading to a 6-term error procedure, in analysers restricted to forward transmission only, whereas 12 error terms must be found by repeating the 6-term calibration in reverse connection in reversing test sets. After calibration, normal measurement of the DUT S-parameters can proceed, and their raw values corrected by means of an explicit expression, stated but not proved in eqns. 5.7—5.10, in terms of the measured

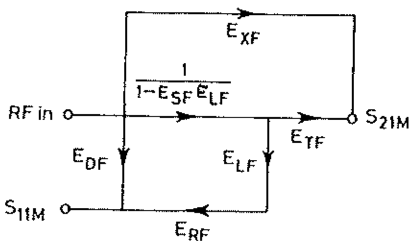

Fig. 5.9 *Topographical reduction*

S-parameters and errors found during calibration[3]:

$$S_{11} = \frac{(1 + DE_{SR})A - E_{LF}BC}{(1 + AE_{SF})(1 + DE_{SR}) - CBE_{LR}E_{LF}} \tag{5.7}$$

$$S_{12} = \frac{[1 + A(E_{SF} - E_{LR})]C}{(1 + AE_{SF})(1 + DE_{SR}) - CBE_{LR}E_{LF}} \tag{5.8}$$

$$S_{21} = \frac{[1 + D(E_{SR} - E_{LF})]B}{(1 + AE_{SF})(1 + DE_{SR}) - CBE_{LR}E_{LF}} \tag{5.9}$$

$$S_{22} = \frac{(1 + AE_{SF})D - E_{LR}BC}{(1 + AE_{SF})(1 + DE_{SR}) - CBE_{LR}E_{LF}} \tag{5.10}$$

with

$$A = (S_{11M} - E_{DF})/E_{RF} \qquad B = (S_{21M} - E_{XF})/E_{TF}$$

$$C = (S_{12M} - E_{XR})/E_{TR} \qquad D = (S_{22M} - E_{DR})/E_{RR}$$

It is clear that all four parameters must first be measured and substituted in the expressions, before a corrected version of any one of them can be calculated.

An algorithm[3] of the experimental procedure, in Fig. 5.10, begins with calibration of the test set, either for four or two parameters, depending on whether DUT reversal is necessary. Crosstalk, not shown, should also be measured, so that the flow chart becomes universal in the sense that by repeating the six coefficients derived for the 'one path' calibration, or by retaining all 12 coefficients for a 'two-path', either case can be calculated.

An example of an earlier non-switching test set, this time for a transmission measurement, is given in Fig. 5.11, to illustrate how operator involvement depends on the degree of automation. The harmonic convertor contains a sampling mixer with step-recovery diode, and gives an output at 20 MHz to the analyser. Electrical or manual adjustment of the reference-line length and DUT reversal are operator tasks, as are the considerable re-arrangements necessary to convert the test set to a reflection form illustrated in Fig. 5.12. Consequent cable movement, connector wear and component changes lead to increased error, in contrast to the static arrangement in the HP8510. Automatic performance of these tasks reduces measurement time, increases repeatability and accuracy, but also de-skills the operator, with increased equipment costs offset against cheaper labour.

For waveguide measurements, the two test sets can be realised by a waveguide network of the type illustrated[7] in Fig. 5.13. Waveguide size depends on frequency, giving very large layouts at low frequencies. Accuracy is maintained by splitting the sweeper input between two nearly identical waveguide paths and by selecting couplers in matched pairs. Fixed and sliding short circuits

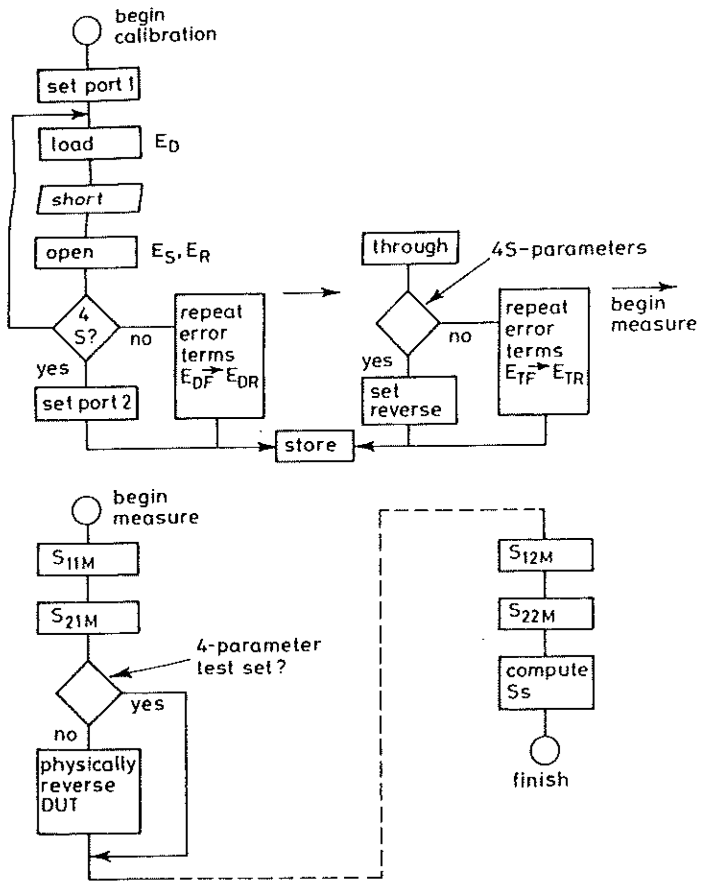

Fig. 5.10 *Algorithm for calibration and test*

reflect equal signals into the two channels via 10 dB directional couplers to allow transmission tests. Added waveguide in the reference channel cancels the DUT phase path. A reflection test is made by replacing the fixed short circuit with the DUT, and placing through connections in reference and test channels.

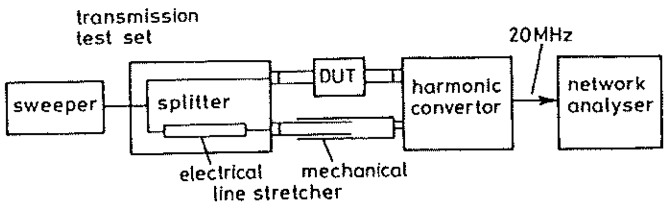

Fig. 5.11 *Coaxial transmission test set*

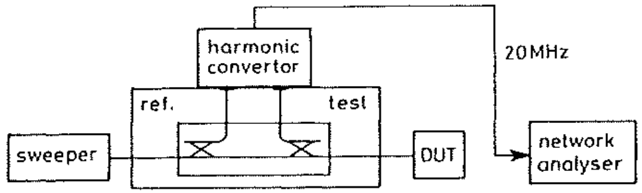

Fig. 5.12 *Coaxial reflection test set*

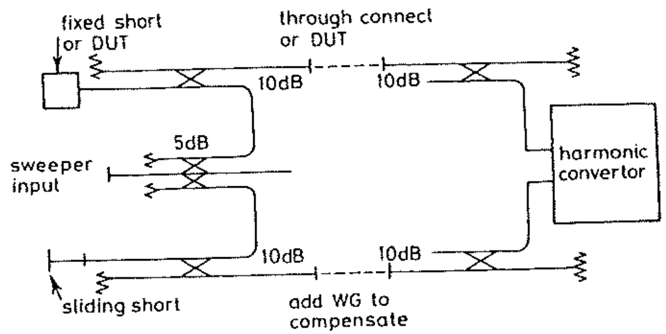

Fig. 5.13 *Waveguide reflection/transmission test set*

In both cases line stretching is possible in the reference channel by movement of the sliding short circuit, and error correction can be applied exactly as in the coaxial case.

5.4 Signal detection

The HP8510, in common with many other network analysers, is based on harmonic mixing with local-oscillator retuning and tracking to ensure accurate phase comparison and a dynamic range from 80 to 100 dB over a wide frequency band from 45 MHz to 26·5 GHz. Network analysers with fundamental mixing, illustrated[5] in Fig. 5.14, have wider dynamic ranges in excess of 100 dB, but are limited by a down-conversion process to an upper frequency not much above 2 GHz. In the example shown, beating between a swept and two fixed sources causes the local oscillator to track the split RF signal in a range 0·5—1300 MHz by a fixed amount equal to the intermediate frequency. Narrow IF bandwidth (10 kHz) and lack of spurious and harmonic responses, give sensitivities of −110 dBm. The two IF outputs are often synchronously detected before being processed for display.

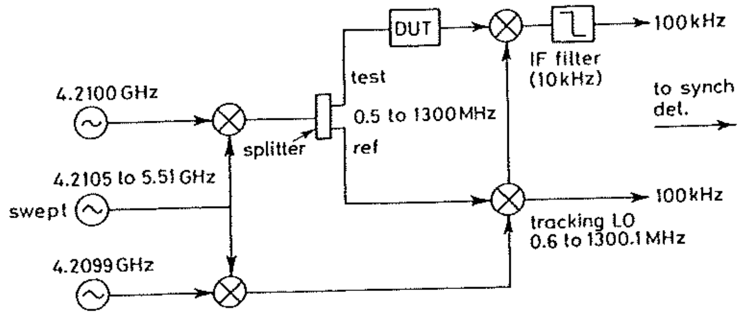

Fig. 5.14 *Fundamental mixing*

5.5 Synchronous detection

Output of simultaneous reflection and transmission data from the two synchronous detectors in the HP8510 is digitised for computer processing, whereas in earlier analysers results remain in analogue form prior to display. There are two mixers in a synchronous detector, each connected to both the test and reference signals but with a quadrature phase shift in the test signal as shown in Fig. 5.15. If $R \cos \omega t$ is the reference and $T \cos \omega t$ is the test signal, output from mixer A is

$$X = R \cos (\omega t)\, T \cos (\omega t + \phi) \tag{5.11}$$

and from B

$$Y = R \cos (\omega t + 90)\, T \cos (\omega t + \phi) \tag{5.12}$$

These become, after low-pass filtering,

$$X = M \cos \phi \tag{5.13}$$

$$Y = M \sin \phi \tag{5.14}$$

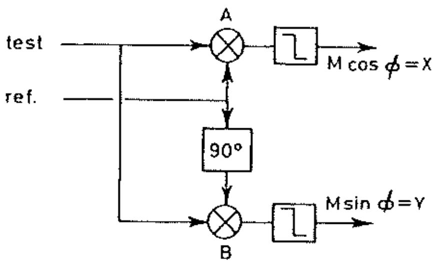

Fig. 5.15 *Synchronous detection*

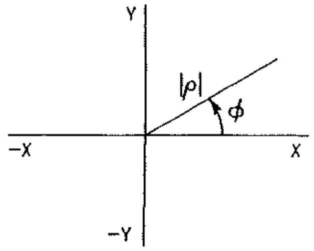

Fig. 5.16 *Polar display*
$\rho \propto \sqrt{(X^2 + Y^2)}$
$\phi = \tan^{-1} (Y/X)$

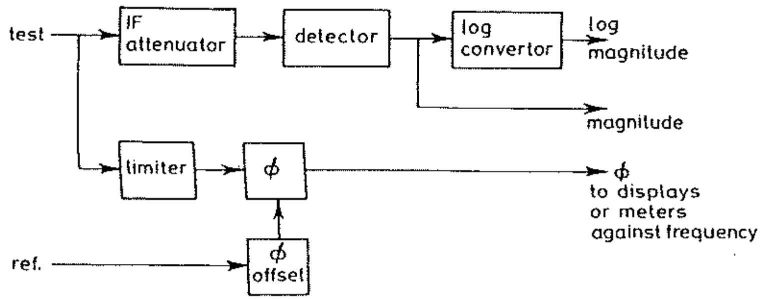

Fig. 5.17 *Magnitude and phase display*

where M is proportional to the test amplitude since, in the product $M = RT$, common-mode variations have been cancelled. Orthogonal display of X and Y produces a polar plot of the complex transmission ratio through the DUT with amplitude proportional to $\sqrt{X^2 + Y^2}$ and phase angle $\phi = \tan^{-1} (Y/X)$, as illustrated in Fig. 5.16. Polar plots are often displayed with a Smith chart, either in overlay or computer-generated form.

An alternative display of amplitude and phase on meters or an oscillosope is sometimes preferred, and Fig. 5.17 in block-diagram form shows how this can be realised in analogue circuits, with frequency proportional to the horizontal scan of a dynamic vertical display of amplitude or phase, or with all three indicated statically on meters.

5.6 Computer control

In the HP8510 complex signal components enter a sample-and-hold output multiplier prior to A/D conversion. All data processing and displays are performed by computer to provide a wide choice of display formats (log, dB,